Inorg. Chem. **XXXX**, *xx*, 0

Inorganic Chemistry
Article

Coordination Cages of Rhodium and Iridium as Exoreceptors for Alkali Metal Ions

Sebastian Mirtschin, Elvira Krasniqi, Rosario Scopelliti, and Kay Severin*

Institut des Sciences et Ingénierie Chimiques, École Polytechnique Fédérale de Lausanne (EPFL), CH-1015 Lausanne, Switzerland

Received March 10, 2008

Hexanuclear coordination cages of the formula $[(C_5Me_4R)M(C_7H_3NO_4)]_6$ (M = Rh, Ir; R = Me, H) were obtained by stepwise reaction of $[(C_5Me_4R)MCl_2]_2$ with, first, AgOAc and, then, pyridine-3,5-dicarboxylic acid. Crystallographic analyses show that the cages adopt a distorted octahedral geometry with the pyridine-3,5-dicarboxylates functioning as dianionic, bridging ligands, each of which connects three different $(C_5Me_4R)M$ fragments. The cages act as exoreceptors for the large alkali metal ions K^+ and Cs^+ but show low affinity for Na^+. Crystallographic and NMR spectroscopic analyses indicate that two metal ions can be coordinated to the surface of the cages. The respective binding sites comprise three carbonyl O-atoms from the bridging pyridine-3,5-dicarboxylate ligand.

Introduction

The utilization of transition metal-based self-assembly processes has emerged as one of the most efficient ways to build artificial molecular cages.[1] Typically, a metal complex with two or more available coordination sites is reacted with an appropriately designed multifunctional ligand to give the cage in one step in high yield. An impetus for studying such coordination cages is the realization that these compounds can display fascinating host−guest chemistry. The group of Fujita, for example, has described a Pd^{II}-based cage, which can act as a sequence-selective receptor for peptides[2] or which can stabilize highly reactive species such as the coordinatively unsaturated manganese complex $[(\eta^5\text{-}C_5H_4Me)Mn(CO_2)]$.[3] Another example is the recent work of Pluth, Raymond, and Bergman, who have shown that encapsulation in tetranuclear coordination cages can change the pK_a of guests by more than four units.[4]

Investigations about the host−guest chemistry of coordination cages have focused almost exclusively on binding of guests in the interior of the cage. However, there are some first studies about molecular recognition events on the surface of cages. Fujita et al. have functionalized a dodecanuclear palladium cage with saccharides. The sugar-coated cage was found to bind to the lectins concanavalin A and peanut agglutinin.[5] Raymond and co-workers have shown for a tetrahedral gallium cage that exohedral guests can modify the exchange kinetics of encapsulated guests.[6] The binding of ammonium ions to the surface of anionic cages was demonstrated by the group of Saalfrank,[7] and the association of triflate anions to the exterior of a cationic palladium cage

* To whom correspondence should be addressed. E-mail: kay.severin@epfl.ch.

(1) For recent reviews see (a) Maurizot, V.; Yoshizawa, M.; Kawano, M.; Fujita, M. *Dalton Trans.* **2006**, 2750–2756. (b) Cronin, L. *Angew. Chem., Int. Ed.* **2006**, *45*, 3576–3578. (c) Kleij, A. W.; Reek, J. N. H. *Chem.—Eur. J.* **2006**, *12*, 4218–4227. (d) Amijs, C. H. M.; van Klink, G. P. M.; van Koten, G. *Dalton Trans.* **2006**, 308–327. (e) Fiedler, D.; Leung, D. H.; Bergman, R. G.; Raymond, K. N. *Acc. Chem. Res.* **2005**, *38*, 349–358. (f) Fujita, M.; Tominaga, M.; Hori, A.; Therrien, B. *Acc. Chem. Res.* **2005**, *38*, 369–378. (g) Schmittel, M.; Kalsani, V. *Top. Curr. Chem.* **2005**, *245*, 1–53. (h) Hamilton, T. D.; MacGillivray, L. R. *Cryst. Growth Des.* **2004**, *4*, 419–430. (i) Seidel, S. R.; Stang, P. J. *Acc. Chem. Res.* **2002**, *35*, 972–983.

(2) Tashiro, S.; Tominaga, M.; Kawano, M.; Therrien, B.; Ozeki, T.; Fujita, M. *J. Am. Chem. Soc.* **2005**, *127*, 4546–4547.

(3) Kawano, M.; Kobayashi, Y.; Ozeki, T.; Fujita, M. *J. Am. Chem. Soc.* **2006**, *128*, 6558–6559.

(4) (a) Pluth, M. D.; Bergman, R. G.; Raymond, K. N. *Science* **2007**, *316*, 85–88. (b) Pluth, M. D.; Bergman, R. G.; Raymond, K. N. *J. Am. Chem. Soc.* **2007**, *129*, 11459–11467.

(5) Kamiya, N.; Tominaga, M.; Sato, S.; Fujita, M. J. *Am. Chem. Soc.* **2007**, *129*, 3816–3817.

(6) Davis, A. V.; Fiedler, D.; Seeber, G.; Zahl, A.; van Eldik, R.; Raymond, K. N. *J. Am. Chem. Soc.* **2006**, *128*, 1324–1333.

(7) (a) Saalfrank, R. W.; Demleitner, B.; Glaser, H.; Maid, H.; Reihs, S.; Bauer, W.; Maluenga, M.; Hampel, F.; Teichert, M.; Krautscheid, H. *Eur. J. Inorg. Chem.* **2003**, 822–829. (b) Saalfrank, R. W.; Burak, R.; Reihs, S.; Löw, N.; Hampel, F.; Stachel, H.-D.; Lentmaier, J.; Peters, K.; Peters, E.-M.; von Schnering, H. G. *Angew. Chem., Int. Ed. Engl.* **1995**, *34*, 993–995. (c) Saalfrank, R. W.; Stark, A.; Bremer, M.; Hummel, H.-U. *Angew. Chem., Int. Ed. Engl.* **1990**, *29*, 311–314. (d) Saalfrank, R. W.; Stark, A.; Peters, K.; von Schnering, H. G. *Angew. Chem., Int. Ed. Engl.* **1988**, *7*, 851–853.

10.1021/ic800410x CCC: $40.75
Published on Web 06/20/2008

Scheme 1

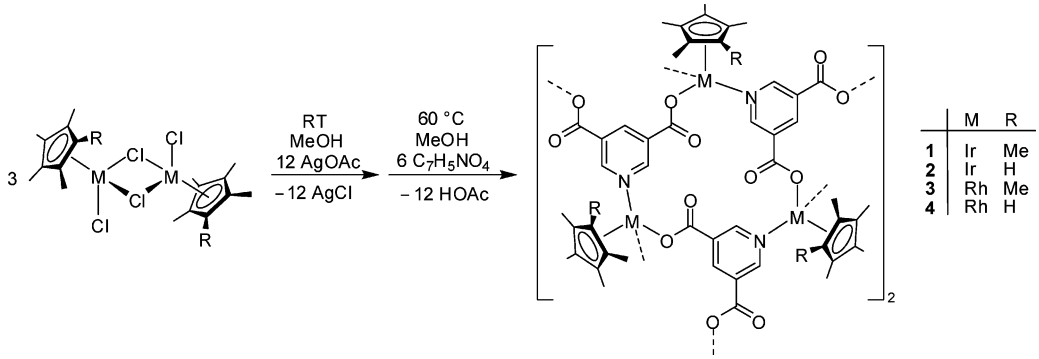

was described by Dalcanale, Macchioni, et al.[8] Recently, Atwood et al. have reported that it is possible to perform ligand exchange reactions at the metal periphery of a zinc-seamed pyrogallol[4]arene cage.[9] The ligand exchange was found to have an effect on the electronic communication between the cage and an endobound 3-methylpyridine guest. These reports are first evidence that coordination cages can exhibit interesting exohedral chemistry.[10] Below we describe further investigations along these lines. The syntheses and the structures of hexanuclear cages containing (cyclopentadienyl)M^{III} complexes (M = Rh, Ir) are reported. The cages were found to act as ditopic exoreceptors for the large alkali metal ions K^+ and Cs^+.

Results and Discussion

The utilization of the organometallic Cp^*Rh^{III} fragment as a building block for the construction of coordination cages was first reported by Rauchfuss et al.[11] They found that cyanide can be employed as a bridging ligand to build cubic structures of the general formula $[\{Cp^*Rh(\mu\text{-}CN)_3\}_4(ML_n)_4]^x$.[12] Interestingly, the cyanometallate $[\{Cp^*Rh(\mu\text{-}CN)_3\}_4\{Mo(CO)_3\}_4]^{4-}$ acts as a selective endoreceptor for the Cs^+ ion.[13] More recently, we and others have shown that Cp*Rh and Cp*Ir complexes can be combined with multifunctional ligands to build 3-dimensional structures such as metallocryptands,[14] expanded helicates,[15] boxes,[16] and metalloprisms.[17] In continuation of our studies about the supramolecular chemistry of organometallic half-sandwich complexes,[18] we have investigated the reaction of the rhodium and iridium complexes $[(C_5Me_4R)MCl_2]_2$ (M = Rh, Ir; R = Me, H) with the trifunctional ligand pyridine-3,5-dicarboxylic acid. This study was stimulated by our recent finding that pyridine-3,5-dicarboxylic acid can be used to prepare a hexanuclear ruthenium cage of the formula $[(cymene)Ru(C_7H_3NO_4)]_6$.[19] NMR titration experiments with KOAc had suggested that the cage is able to act as a host for K^+. More detailed investigations about the host−guest chemistry were unfortunately hampered by the fact that the ruthenium cage underwent a K^+ induced rearrangement. We were thus interested whether it is possible to prepare analogous cyclopentadienyl rhodium and/or iridium complexes.

Screening several solvents and activation methods, we found that a two-step procedure, with initial activation of $[(C_5Me_4R)MCl_2]_2$ by AgOAc followed by reaction with pyridine-3,5-dicarboxylic acid, resulted in the precipitation of the desired cage complexes **1**−**4** in good yields (Scheme 1). The reaction with AgOAc was expected to give the known acetate complexes $(C_5Me_4R)M(OAc)_2$.[20] The latter were not isolated but directly reacted with the pyridine ligand after removal of AgCl.

The NMR spectra of the complexes **1**−**4** in $CDCl_3$ showed a single set of signals for the π-ligands, as well as for the bridging pyridine-3,5-dicarboxylate ligands. A characteristic feature was the reduced symmetry of the latter when compared to the free ligand: the ^1H NMR spectra showed three distinct signals for the three aromatic protons, and the ^{13}C NMR spectra displayed five signals for the aromatic C-atoms and two signals for carboxylate groups.

To obtain decisive information about the nuclearity of the complexes, single crystal X-ray analyses were carried out for all four complexes. The molecular structures of **1**−**4** are very similar, and graphic representations are only given for

(8) Zuccaccia, D.; Pirondini, L.; Pinalli, R.; Dalcanale, E.; Macchioni, A. *J. Am. Chem. Soc.* **2005**, *127*, 7025–7032.
(9) Power, N. P.; Dalgarno, S. J.; Atwood, J. L. *Angew. Chem., Int. Ed.* **2007**, *46*, 8601–8604.
(10) For the surface chemistry of polyoxomolybdate capsules see (a) Merca, A.; Haupt, E. T. K.; Mitra, T.; Bögge, H.; Rehder, D.; Müller, A. *Chem.—Eur. J.* **2007**, *13*, 7650–7658. (b) Müller, A.; Toma, L.; Bögge, H.; Schäffer, C.; Stammler, A. *Angew. Chem., Int. Ed.* **2005**, *44*, 7757–7761.
(11) Klausmeyer, K. K.; Rauchfuss, T. B.; Wilson, S. R. *Angew. Chem., Int. Ed.* **1998**, *37*, 1694–1696.
(12) For a review see. Boyer, J. L.; Kuhlman, M. L.; Rauchfuss, T. B. *Acc. Chem. Rev.* **2007**, *40*, 233–242.
(13) Klausmeyer, K. K.; Wilson, S. R.; Rauchfuss, T. B. *J. Am. Chem. Soc.* **1999**, *121*, 2705–2711.
(14) Amori, H.; Rager, M. N.; Cagnol, F.; Vaissermann, J. *Angew. Chem., Int. Ed.* **2001**, *40*, 3636–3683.
(15) Grote, Z.; Bonazzi, S.; Scopelliti, R.; Severin, K. *J. Am. Chem. Soc.* **2006**, *128*, 10328–10383.
(16) Han, Y.-F.; Lin, Y.-J.; Weng, L.-H.; Berke, H.; Jin, G.-X. *Chem. Commun.* **2008**, 350–352.
(17) (a) Han, Y.-F.; Jia, W.-G.; Lin, Y.-J.; Jin, G.-X. *J. Organomet. Chem.* **2008**, *693*, 546–550. (b) Govindaswamy, P.; Lindner, D.; Lacour, J.; Süss-Fink, G.; Therrien, B. *Dalton Trans.* **2007**, 4457–4463. (c) Han, Y.-F.; Lin, Y.-J.; Jia, W.-G.; Weng, L.-H.; Jin, G.-X. *Organometallics* **2007**, *26*, 5848–5853. (d) Govindaswamy, P.; Süss-Fink, G.; Therrien, B. *Inorg. Chem. Commun.* **2007**, *10*, 1489–1492.
(18) (a) Severin, K. *Chem. Commun.* **2006**, 3859–3867. (b) Severin, K. *Coord. Chem. Rev.* **2003**, *245*, 3–10.
(19) Brasey, T.; Scopelliti, R.; Severin, K. *Chem. Commun.* **2006**, 3308–3310.
(20) Kang, J. W.; Maitlis, P. M. *J. Organomet. Chem.* **1971**, *30*, 127–133.

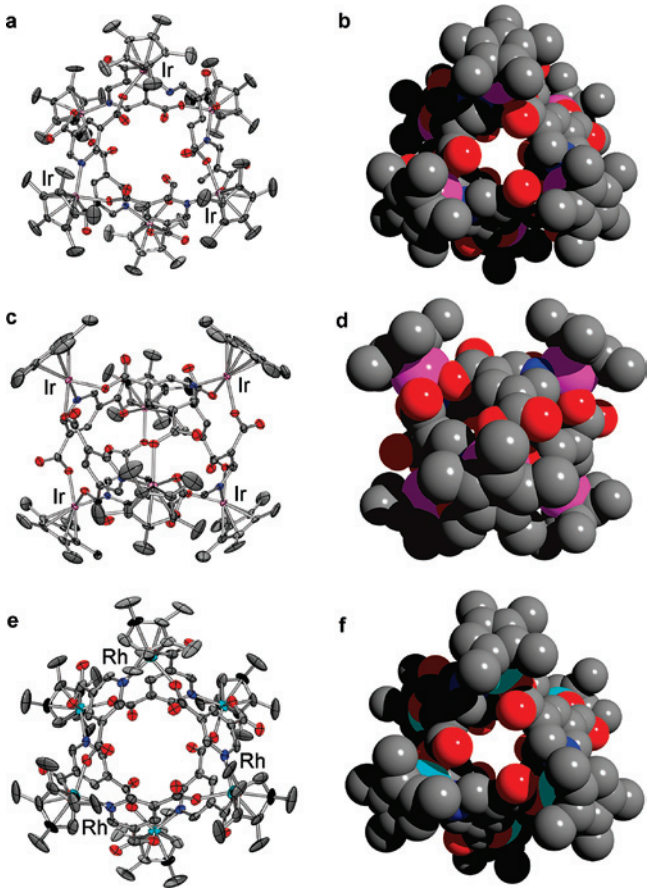

Figure 1. Molecular structures of the complexes **1** and **4** in the crystal. The graphics a−d show complex **1** in an ORTEP representation along the C_3 axis (a), the same view in space filling representation (b), ORTEP representation from the side (c), and the same view in space filling representation (d). The graphics e and f show complex **4** in an ORTEP representation along the C_3 axis (e), and the same view in space filling representation (f). Hydrogen atoms and co-crystallized solvent molecules are not shown for clarity. The thermal ellipsoids are set at 50% probability.

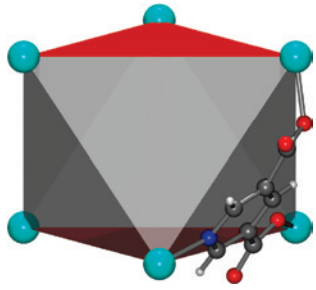

Figure 2. Coordination cages **1**−**4** can be described as trigonal antiprisms, in which the metals occupy the six vertices, and the bridging ligands, six out of the eight triangular faces (the graphic is based on the atom coordinates of complex **3**).

the complexes **1** and **4** (Figure 1). In all cases, six $(C_5Me_4R)M$ fragments are connected by six pyridine-3,5-dicarboxylate ligands. The latter are coordinated to three metal centers via two carboxylate O-atoms and the pyridine N-atom. All four cages show crystallographic C_{3i} symmetry. The metals are positioned in the corner of distorted trigonal antiprisms with diagonal lengths of approximately 11.7 Å (M···M distance). Six out of the eight triangular faces of the antiprism are occupied by the bridging ligands (Figure 2). The remaining two faces have a small opening, which is

Scheme 2

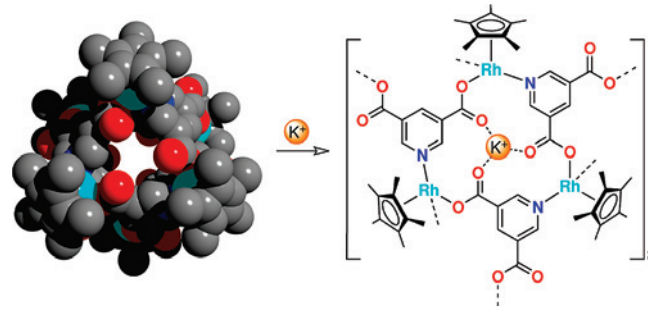

surrounded by carbonyl groups. The cavities of the cages are likely filled with disordered solvent molecules (see the Experimental Section for further details). For the complexes **1**, **3**, and **4**, additional six methanol molecules are found around each cage. They are within a hydrogen bond distance to carbonyl groups of the bridging pyridine-3,5-dicarboxylate ligands (**1**, O···O = 2.727(10) Å; **3**, O···O = 2.718(9) Å; **4**, O···O = 2.699(16) Å).

Half of the carbonyl O-atoms of the bridging pyridine-3,5-dicarboxylate ligand are positioned in close proximity to each other (O···O ∼ 4.2 Å). The complexes therefore display two potential binding sites for oxophilic metal ions (for complex **3** and K^+ this situation is shown in Scheme 2).

To evaluate the host properties of the respective cages, NMR titrations were performed with NaF, KF, and CsF in a 1:1 mixture of CD_3OD and d_8-toluene. For the potassium

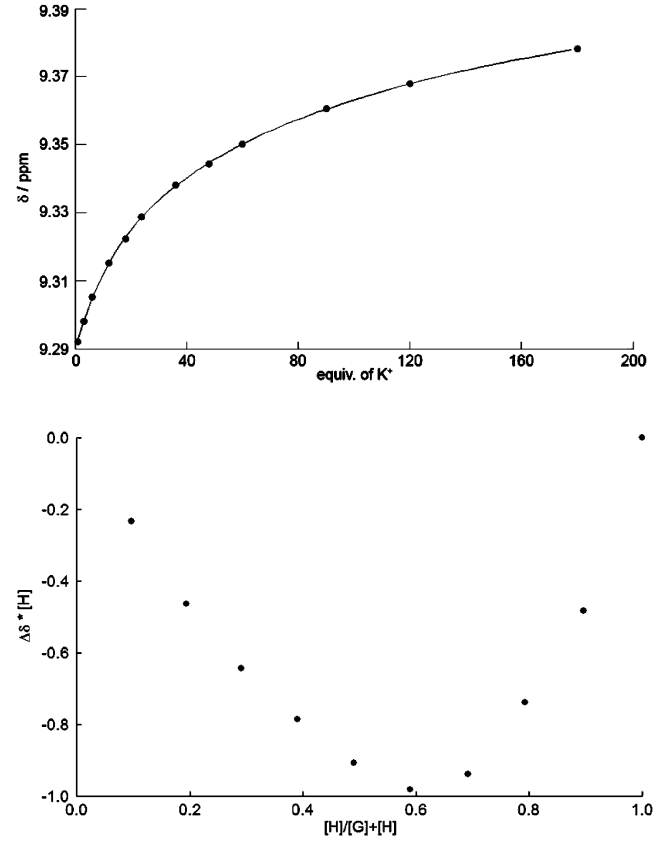

Figure 3. Top: Binding isotherm for the complexation of K^+ (0.10−18.0 mM) to receptor **3** (0.10 mM). The line was obtained by fitting the data to a 2:1 binding model. Bottom: Job plot for the complexation of K^+ to receptor **3**.

Table 1. Binding Constants for the Complexation of K^+ and Cs^+ by the Complexes 1−4[a]

entry	host	cation	anion	K_1 [M^{-1}]	K_2 [M^{-1}]
1	$[Cp^*Ir(C_7H_3NO_4)]_6$ (**1**)	K^+	F^-	2.7 (±0.6) × 10^2	61 (±6)
2	$[Cp^*Ir(C_7H_3NO_4)]_6$ ($\mathbf{1}_t$)	Cs^+	F^-	2.7 (±0.4) × 10^2	23 (±5)
3	$[(C_5Me_4H)Ir(C_7H_3NO_4)]_6$ (**2**)	K^+	F^-	1.6 (±0.5) × 10^2	27 (±4)
4	$[(C_5Me_4H)Ir(C_7H_3NO_4)]_6$ (**2**)	Cs^+	F^-	1.9 (±0.4) × 10^2	14 (±2)
5	$[Cp^*Rh(C_7H_3NO_4)]_6$ (**3**)	K^+	F^-	4.3 (±0.4) × 10^2	36 (±2)
6	$[Cp^*Rh(C_7H_3NO_4)]_6$ (**3**)	Cs^+	F^-	6.1 (±1.1) × 10^2	21 (±2)
7	$[(C_5Me_4H)Rh(C_7H_3NO_4)]_6$ (**4**)	K^+	F^-	2.3 (±0.7) × 10^2	57 (±1)
8	$[(C_5Me_4H)Rh(C_7H_3NO_4)]_6$ (**4**)	Cs^+	F^-	2.0 (±0.5) × 10^2	24 (±6)
9	$[Cp^*Rh(C_7H_3NO_4)]_6$ (**3**)	K^+	$CF_3CO_2^-$	5.6 (±0.4) × 10^2	46 (±1)

[a] The binding constants were calculated by fitting the data of NMR titration experiments performed in 1:1 mixture of CD_3OD and d_8-toluene as described in the experimental section.

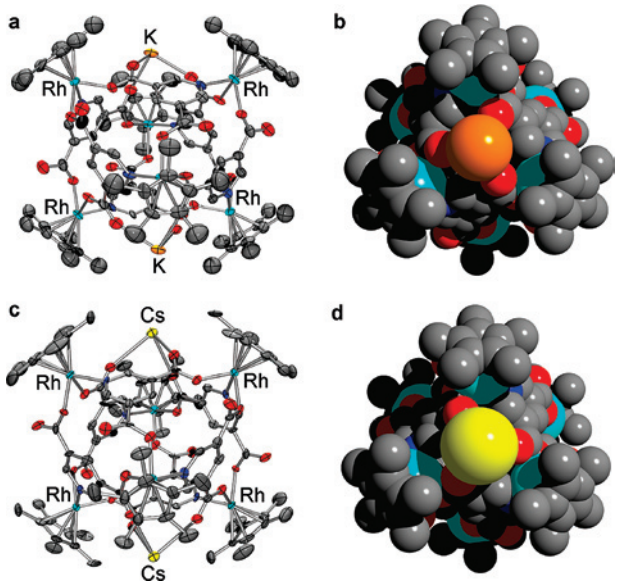

Figure 4. Molecular structures of **5** and **6** in the crystal. The graphics a and b show the K^+ adduct in an ORTEP representation with view from the side (a), and in space filling representation with view along the C_3 axis (b). The graphics c and d show the Cs^+ adduct in an ORTEP representation with view from the side (c), and in space filling representation with view along the C_3 axis (d). Hydrogen atoms, co-crystallized solvent molecules, and counteranions are not shown for clarity. The thermal ellipsoids are set at 40% probability.

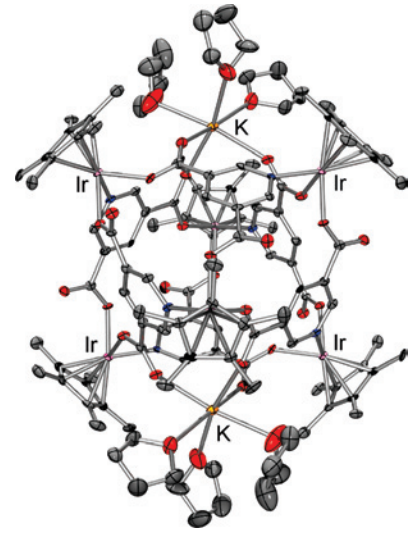

Figure 5. ORTEP representation of the molecular structure of the $K(BPh_4)$ adduct **7** in the crystal. Hydrogen atoms, BPh_4^- anions, and nonbound THF molecules inside and outside the cage are not shown for clarity. The thermal ellipsoids are set at 40% probability.

and cesium salt, complexation induced shifts of up to 0.19 ppm were observed for the signals of the bridging pyridine-3,5-dicarboxylate ligands (Figure 3). The addition of NaF, on the other hand, gave only minor shifts indicating a very weak interaction with the cages. For KF and CsF, the resulting binding isotherms were fitted to a 2:1 binding model. For the interaction of the Cp*Rh complex **3** with KF, this stoichiometry was confirmed by a Job plot[21] analysis (Figure 3). In addition, we have measured high resolution ESI-MS spectra of the K^+ and Cs^+ adducts of complex **3**, which showed peaks for the 2:1 complexes.

The binding constants obtained from the NMR titration experiments are summarized in Table 1. The values for the first binding constant K_1 vary between 1.6 × 10^2 M^{-1} to 6.1 × 10^2 M^{-1}. The differences between the complexes are small but for a given cation, the Rh complexes **3** and **4** (entries 5−8) show a slightly higher binding affinity than the Ir complexes **1** and **2** (entries 1−4). Furthermore, the Cp*M complexes are slightly more potent receptors than the $(C_5Me_4H)M$ complexes. The NMR titrations were performed with the fluoride salts because they display a reasonable solubility in the methanol/toluene mixture, which was employed to dissolve the cages. Titration with $K(CF_3CO_2)$ instead of KF gave similar but not identical binding constants (entry 9 vs entry 5) indicating a small anion effect on binding.

To obtain more detailed information about the binding mode of the alkali metal ions, we have crystallized the cages in the presence of an excess of MF salts ($M^+ = K^+$, Cs^+). Suitable single crystals for a crystallographic analysis were obtained for the KF adduct **5** and the CsF adduct **6**. In agreement with the NMR spectroscopic studies, the crystallographic analyses revealed that two alkali metal ions are bound to the cages via the three adjacent carbonyl groups (Figure 4).

The complexation of K^+ and Cs^+ to cage **3** results in minor structural changes. The metal−metal distance of the opposite Rh atoms is slightly expanded from 11.703(2) Å for **3** to an average of 11.83 Å for **5** and 11.73 Å for **6**. Somewhat larger deviations are observed for the three carbonyl O-atoms, which constitute the alkali metal ion binding sites: whereas an O···O distance of 4.110(8) Å is observed for **3**, an average distance of 3.92 Å is found for the K^+ adduct **5** and a distance of 3.99 Å for the Cs^+ adduct **6**. The average $K^+ \cdots O_{cage}$ distance in **5** of 2.74 Å is similar to what has

(21) Schneider, H.-J.; Yatasimirsky, A. K., *Principles and Methods in Supramolecular Chemistry*; Wiley: Chichester, 2000, Chapter D.

Table 2. Crystallographic Data for the Complexes **1**, **2**, and **3**

	1 × 6MeOH	**2**	**3** × 6MeOH
empirical formula	$C_{108}H_{132}Ir_6N_6O_{30}$	$C_{96}H_{96}Ir_6N_6O_{24}$	$C_{108}H_{132}N_6O_{30}Rh_6$
mol. weight/g mol^{-1}	3147.40	2870.99	2611.66
crystal size/mm^3	0.48 × 0.40 × 0.36	0.47 × 0.40 × 0.37	0.30 × 0.28 × 0.20
crystal system	rhombohedral	rhombohedral	rhombohedral
space group	$R\bar{3}$	$R\bar{3}$	$R\bar{3}$
a/Å	24.0983(3)	23.3090(3)	24.1442(5)
b/Å	24.0983(3)	23.3090(3)	24.1442(5)
c/Å	18.1977(3)	18.8741(3)	18.1743(6)
α/°	90	90	90
β/°	90	90	90
γ/°	120	120	120
volume/Å^3	9152.1(2)	8880.6(2)	9175.2(4)
Z	3	3	3
density/g cm^{-3}	1.713	1.610	1.418
temperature/*K*	140(2)	140(2)	140(2)
absorption coeff./mm^{-1}	6.589	6.779	0.862
Θ range/°	2.81 to 26.37	2.88 to 26.36	2.81 to 25.02
index ranges	−30 → 29, −30 → 30, −18 → 22	−29 → 28, −29 → 28, −23 → 23	−27 → 28, −28 → 28, −21 → 19
reflections collected	26208	25358	18155
data/restraints/param.	4147/132/301	4044/132/262	3583/0/226
goodness-of-fit on F^2	1.144	1.104	1.069
final *R* indices [$I > 2\sigma(I)$]	$R1 = 0.0249$, $wR2 = 0.0695$	$R1 = 0.0333$, $wR2 = 0.0745$	$R1 = 0.0603$, $wR2 = 0.1481$
R indices (all data)	$R1 = 0.0371$, $wR2 = 0.0787$	$R1 = 0.0443$, $wR2 = 0.0836$	$R1 = 0.0860$, $wR2 = 0.1645$

Table 3. Crystallographic Data for the Complexes **4**, **5**, and **6**

	4 × 6MeOH	**5** × 12MeOH	**6** × 12MeOH
empirical formula	$C_{102}H_{120}N_6O_{30}Rh_6$	$C_{114}H_{156}K_2N_6O_{36}Rh_6$	$C_{114}H_{156}Cs_2N_6O_{36}Rh_6$
mol. weight/g mol^{-1}	2527.50	2882.11	3069.73
crystal size/mm^3	0.52 × 0.29 × 0.25	0.26 × 0.16 × 0.09	0.37 × 0.30 × 0.23
crystal system	rhombohedral	triclinic	triclinic
space group	$R\bar{3}$	$P\bar{1}$	$P\bar{1}$
a/Å	23.693(3)	15.233(2)	15.2318(5)
b/Å	23.693(3)	15.258(2)	15.2858(4)
c/Å	18.286(4)	18.261(6)	18.3701(5)
α/°	90	72.04(2)	65.906(3)
β/°	90	66.871(15)	71.991(3)
γ/°	120	76.063(12)	74.721(3)
volume/Å^3	8890(3)	3677.7(14)	3666.44(18)
Z	3	1	1
density/g cm^{-3}	1.416	1.301	1.390
temperature/*K*	100(2)	100(2)	140(2)
absorption coeff./mm^{-1}	0.887	0.781	1.216
Θ range/°	3.44 to 25.01	3.31 to 22.98	2.57 to 25.03
index ranges	−28 → 28, −28 → 28, −21 → 21	−16 → 16, −16 → 16, −20 → 20	−17 → 18, −18 → 18, −21 → 21
reflections collected	50616	42789	30201
data/restraints/param.	3491/74/281	10072/252/740	12851/144/739
goodness-of-fit on F^2	1.211	1.064	1.044
final *R* indices [$I > 2\sigma(I)$]	$R1 = 0.0689$, $wR2 = 0.1555$	$R1 = 0.1045$, $wR2 = 0.2524$	$R1 = 0.0629$, $wR2 = 0.1647$
R indices (all data)	$R1 = 0.0810$, $wR2 = 0.1613$	$R1 = 0.1869$, $wR2 = 0.2913$	$R1 = 0.1098$, $wR2 = 0.1994$

been observed for [(18-crown-6) × K^+] complexes with $K^+\cdots O$ distances in the range of 2.74 to 2.85 Å.[22] The average $Cs^+\cdots O_{cage}$ distance for **6** is 3.02 Å.

The three remaining sites of the hexa-coordinated M^+ ions in **5** and **6** are occupied with highly disordered, O-bound methanol. As it was observed for the free hosts **1**, **3**, and **4**, six additional MeOH molecules are found around **5** and **6**. They are within a hydrogen bond distance to carbonyl groups of the bridging pyridine-3,5-dicarboxylate ligands ($O\cdots O$ = 2.72−3.00 Å). Unfortunately, it was not possible to locate the fluoride counterions (see the experimental part for further details).

To avoid crystallographic problems with fluoride anions, we crystallized the cages with an excess of $M(BPh_4)$ salts ($M^+ = K^+$, Cs^+). For the $K(BPh_4)$ adduct of cage **1** (**7**), we were able to obtain single crystals of sufficient quality for a crystallographic analysis. As observed before, two K^+ ions were coordinated to the coordination cage via the carbonyl groups of the bridging ligand (average $K^+\cdots O$ distance = 2.69 Å). The coordination sphere of the K^+ ions is completed with three THF molecules (average $K^+\cdots O$ distance = 2.76 Å), resulting in a distorted octahedral geometry around the K^+ (Figure 5). The interior of the cage contains one disordered THF molecule.

The ability of the cages **1**−**4** to bind alkali metal ions is reminiscent of what has been observed for 2,3-dihydroxypyridine-based macrocycles of the general formula [(*π*-ligand)$M(C_5H_3NO_2)]_3$ ((*π*-ligand)M = (arene)Ru, (cyclopentadienyl)Rh, (cyclopentadienyl)Ir): three (*π*-ligand)M fragments enclose a binding site that comprises three oxygen atoms of the bridging ligand.[23] Whereas the cages **1**−**4** are selective for the larger cations K^+ and Cs^+, trinuclear macrocycles based on $(C_5Me_4R)M$ fragments were found to be selective for the smaller cations Li^+ and Na^+ (Scheme 3).[23b] This difference can be attributed to the increased size of the binding sites of the cages ($O\cdots O \sim 4.1$ Å) when compared to that of the macrocycles ($O\cdots O \sim 3.1$ Å).

(22) Steed, J. W. *Coord. Chem. Rev.* **2001**, *215*, 171–221.

Table 4. Crystallographic Data for Complex **7**

	7 × 9THF × 4MeOH
empirical formula	$C_{190}H_{236}B_2Ir_6K_2N_6O_{37}$
mol. weight/g mol^{-1}	4448.87
crystal size/mm^3	0.53 × 0.42 × 0.41
crystal system	triclinic
space group	$P\bar{1}$
a/Å	15.287(2)
b/Å	15.890(2)
c/Å	20.760(3)
α/°	107.246(11)
β/°	99.406(14)
γ/°	105.235(19)
volume/Å^3	4484.4(12)
Z	1
density/g cm^{-3}	1.647
temperature/*K*	100(2)
absorption coeff./mm^{-1}	4.557
Θ range/°	3.30 to 25.03
index ranges	−18 → 18, −18 → 18, −24 → 24
reflections collected	76372
data/restraints/param.	15606/40/1117
goodness-of-fit on F^2	1.072
final *R* indices [$I > 2\sigma(I)$]	*R*1 = 0.0512, *wR*2 = 0.1196
R indices (all data)	*R*1 = 0.0707, *wR*2 = 0.1363

Scheme 3

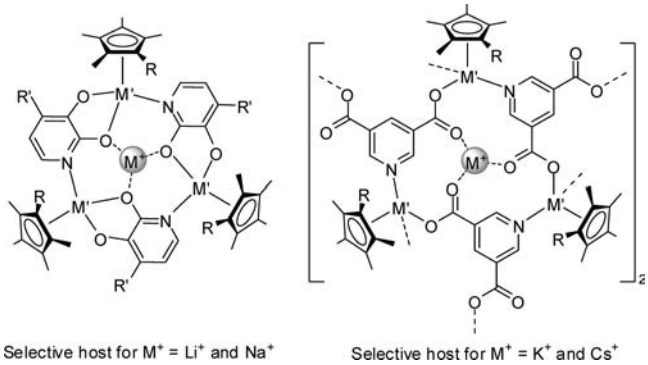

Conclusion

We have described the synthesis and the structures of hexanuclear coordination cages, in which cyclopentadienyl rhodium and iridium complexes are connected by pyridine-3,5-dicarboxylate ligands. The cages act as ditopic exoreceptors for the large alkali metals K^+ and Cs^+ but show low affinity for Na^+. In terms of binding constants, the cages can not rival optimized ionophores such as crown ethers or cryptands.[24] Nevertheless, the affinities are quite respectable given that the binding sites is composed of only three oxygen-donor atoms. Overall, this work is further evidence that coordination cages with interesting exohedral host−guest chemistry can be generated. A perspective is the utilization of such complexes in hierarchical self-assembly processes, in which the organization of coordination cages into nanostructured aggregates is mediated by exohedral guests.

Experimental Section

General. Commercial reagents were purchased from Acros, Fluka or Lancaster and were used as received. The complexes $[Cp^*RhCl_2]_2$,[25] $[Cp^*IrCl_2]_2$,[25] $[(C_5Me_4H)RhCl_2]_2$,[26] and $[(C_5Me_4H)IrCl_2]_2$,[23b] were prepared according to literature procedures. The solvents (analytical grade) were degassed and stored under an atmosphere of dinitrogen. The syntheses were carried out under an atmosphere of dry dinitrogen using standard Schlenk techniques. ^{1}H NMR and ^{13}C-MNMR spectra were recorded on a Bruker 400 MHz spectrometer. Chemical shifts (δ) are reported in parts per million (ppm) and are calibrated relative to solvent residual peaks.

General Procedure for the Synthesis of the Coordination Cages 1−4. The respective half-sandwich complex [(cyclopentadienyl)$MCl_2]_2$ (0.30 mmol) was dissolved in methanol (30 mL). Silver acetate (210 mg, 1.25 mmol) was added, and the resulting mixture was stirred for 2 h at room temperature in the dark. The AgCl precipitate was removed by filtration. A solution of pyridine-3,5-dicarboxylic acid (100 mg, 0.30 mmol) in methanol (4 mL) was then added to the filtrate, and the mixture was stirred for 4 h at 60 °C. After cooling, the product precipitated in the form of an orange or yellow powder, which was collected by filtration, washed with diethyl ether, and dried under vacuum. Crystals were obtained by slow vapor diffusion of diethyl ether into a solution of the respective compound in methanol/toluene (1:1) or chloroform.

$[Cp^*Ir(C_7H_3NO_4)]_6$ (1). Yield: 84%; ^{1}H NMR (400 MHz, CD_3OD/d_8-toluene, 1:1): δ = 9.57 (d, ^4J(H,H) = 2 Hz, 6 H, CCHN), 9.34 (d, ^4J(H,H) = 2 Hz, 6 H, CCHN), 8.21 (t, ^4J(H,H) = 2 Hz, 6 H, CCHC), 1.57 (s, 90 H, CH_3); ^{13}C NMR (100 MHz, CD_3OD/d_8-toluene, 1:1): δ = 171.5, 168.1 (CO_2), 156.3, 154.8, 141.2, 135.2, 135.1 (C, pyridine), 85.3 (C, Cp*), 9.9 (CH_3); elemental analysis calcd (%) for $C_{102}H_{108}Ir_6N_6O_{24}\cdot 2CHCl_3\cdot H_2O$ (3074.3): C 38.89, H 3.51, N 2.62; found: C 38.58, H 3.55, N 2.64.

$[(C_5Me_4H)Ir(C_7H_3NO_4)]_6$ (2). Yield: 65%; ^{1}H NMR (400 MHz, $CDCl_3$): δ = 9.44 (d, ^4J(H,H) = 2 Hz, 6 H, CCHN), 9.03 (d, ^4J(H,H) = 2 Hz, 6 H, CCHN), 8.15 (t, ^4J(H,H) = 2 Hz, 6 H, CCHC), 5.82 (s, 6 H, $C_5(CH_3)_4H$), 1.81 (s, 18 H, $C_5(CH_3)_4H$), 1.79 (s, 18 H, $C_5(CH_3)_4H$), 1.68 (s, 18 H, $C_5(CH_3)_4H$), 1.63 (s, 18 H, $C_5(CH_3)_4H$); ^{13}C NMR (100 MHz, $CDCl_3$): δ = 169.5, 167.7 (CO_2), 155.8, 153.1, 140.9, 135.4, 134.6 (C, pyridine), 91.8, 90.7, 86.4, 85.4, 66.6 (C, Cp*), 11.3, 11.0, 10.3, 9.2 (CH_3); elemental analysis calcd (%) for $C_{96}H_{96}N_6O_{24}Rh_6\cdot CH_3Cl\cdot 3H_2O$ (2975.7): C 38.27, H 3.41, N 2.76; found: C 38.17, H 3.46, N 2.62.

$[Cp^*Rh(C_7H_3NO_4)]_6$ (3). Yield: 84%; ^{1}H NMR (400 MHz, $CDCl_3$): δ = 9.44 (d, ^4J(H,H) = 2 Hz, 6 H, CCHN), 9.11 (d, ^4J(H,H) = 2 Hz, 6 H, CCHN), 8.11 (t, ^4J(H,H) = 2 Hz, 6 H, CCHC), 1.75 (s, 90 H, CH_3); ^{13}C NMR (100 MHz, $CDCl_3$): δ = 171.3, 167.6 (CO_2), 155.2, 153.3, 140.7, 135.1, 134.6 (C, pyridine), 92.8 (d, ^1J(C,Rh) = 9 Hz, C, Cp*), 9.7 (CH_3); elemental analysis calcd (%) for $C_{102}H_{108}N_6O_{24}Rh_6\cdot 6H_2O$ (2527.5): C 48.47, H 4.79, N 3.33; found: C 48.41, H 4.41, N 3.76.

(23) (a) Mimassi, L.; Cordier, C.; Guyard-Duhayon, C.; Mann, B. E.; Amori, H. *Organometallics* **2007**, *26*, 860–864. (b) Grote, Z.; Scopelliti, R.; Severin, K. *J. Am. Chem. Soc.* **2004**, *126*, 16959–16972. (c) Mimassi, L.; Guyard-Duhayon, C.; Rager, M. N.; Amori, H. *Inorg. Chem.* **2004**, *43*, 6644–6649. (d) Grote, Z.; Lehaire, M.-L.; Scopelliti, R.; Severin, K. *J. Am. Chem. Soc.* **2003**, *125*, 13638–13639. (e) Lehaire, M.-L.; Schulz, A.; Scopelliti, R.; Severin, K. *Inorg. Chem.* **2003**, *42*, 3576–3581. (f) Lehaire, M.-L.; Scopelliti, R.; Severin, K. *Angew. Chem., Int. Ed.* **2002**, *41*, 1419–1421. (g) Lehaire, M.-L.; Scopelliti, R.; Severin, K. *Chem. Commun.* **2002**, 2766–2767. (h) Lehaire, M.-L.; Scopelliti, R.; Severin, K. *Inorg. Chem.* **2002**, *41*, 5466–5474. (i) Piotrowski, H.; Severin, K. *Proc. Natl. Acad. Sci.* **2002**, *99*, 4997–5000. (k) Piotrowski, H.; Hilt, G.; Schulz, A.; Mayer, P.; Polborn, K.; Severin, K. *Chem.—Eur. J.* **2001**, *7*, 3196–3208. (l) Piotrowski, H.; Polborn, K.; Hilt, G.; Severin, K. *J. Am. Chem. Soc.* **2001**, *123*, 2699–2700.

(24) (a) Izatt, R. M.; Pawlak, K.; Bradshaw, J. S.; Bruening, R. L. *Chem. Rev.* **1995**, *95*, 2529–2586. (b) Lehn, J.-M. *Acc. Chem. Res.* **1978**, *11*, 49–57.

(25) White, C.; Yates, A.; Maitlis, P. M. *Inorg. Synth.* **1992**, *29*, 228–234.

(26) Bellabarba, R.; Nieuwenhuyzen, M.; Saunders, G. C. *Inorg. Chim. Acta* **2001**, *323*, 78–88.

$[(C_5Me_4H)Rh(C_7H_3NO_4)]_6$ (4). Yield: 78%; ^{1}H NMR (400 MHz, $CDCl_3$): δ = 9.48 (d, ^4J(H,H) = 2 Hz, 6 H, CCHN), 9.00 (d, ^4J(H,H) = 2 Hz, 6 H, CCHN), 8.15 (t, ^4J(H,H) = 2 Hz, 6 H, CCHC), 5.70 (s, 6 H, $C_5(CH_3)_4H$), 1.85 (s, 18 H, $C_5(CH_3)_4H$), 1.83 (s, 18 H, $C_5(CH_3)_4H$), 1.69 (s, 18 H, $C_5(CH_3)_4H$), 1.66 (s, 18 H, $C_5(CH_3)_4H$); ^{13}C NMR (100 MHz, $CDCl_3$): δ = 171.0, 168.4 (CO_2), 155.0, 153.0, 140.8, 135.4, 134.5 (C, pyridine), 100.6 (d, ^1J(C,Rh) = 8 Hz, C, $C_5(CH_3)_4H$), 99.4 (d, ^1J(C,Rh) = 9 Hz, C, $C_5(CH_3)_4H$), 94.5 (d, ^1J(C,Rh) = 8 Hz, C, $C_5(CH_3)_4H$), 85.6 (d, ^1J(C,Rh) = 9 Hz, C, $C_5(CH_3)_4H$), 75.4 (d, ^1J(C,Rh) = 9 Hz, C, $C_5(CH_3)_4H$), 11.2, 10.8, 10.3, 8.8 (CH_3); elemental analysis calcd (%) for $C_{96}H_{96}N_6O_{24}Rh_6 \cdot 5H_2O$ (2425.3): C 47.54, H 4.41, N 3.47; found: C 47.48, H 4.26, N 3.53.

$[\{Cp^*Rh(C_7H_3NO_4)\}_6(KF)_2]$ (5). Crystals of the KF adduct **5** were obtained by vapor diffusion of Et_2O into a solution of complex **3** in toluene/MeOH (1:1) containing an excess of KF.

$[\{Cp^*\ Rh(C_7H_3NO_4)\}_6(CsF)_2]$ (6). Crystals of the CsF adduct **6** were obtained by vapor diffusion of Et_2O into a solution of complex **3** in toluene/MeOH (1:1) containing an excess of CsF.

$[\{Cp^*\ Ir(C_7H_3NO_4)\}_6\{K(BPh_4)\}_2]$ (7). Crystals of the $K(BPh_4)$ adduct **7** were obtained by vapor diffusion of THF into a solution of complex **3** in MeOH containing an excess of $K(BPh_4)$.

High Resolution ESI-MS. Solutions of complex **3** in toluene/MeOH (1:1) containing an excess of KF or CsF were investigated by ESI-MS using an Waters CapLC-coupled Micromass Q-ToF Ultima. The following peaks were observed: *m*/*z* 1264.0635 [**3** + 2 K + $CH_3OH]^{2+}$ (calcd *m*/*z* 1264.0641), *m*/*z* 1358.0010 [**3** + 2 Cs + $CH_3OH]^{2+}$ (calcd *m*/*z* 1358.0052), *m*/*z* 1276.0428 [**3** + Cs + $H]^{2+}$ (calcd *m*/*z* 1276.0433).

Binding Studies. The binding affinities were evaluated by NMR titrations. Titrations were performed in a 1:1 mixture of CD_3OD and d_8-toluene using a host concentration of 0.10 mM with varying amounts of alkali salt. The chemical shifts were analyzed according to a 1:2 binding model, using the nonlinear least-squares curve-fitting program WinEQNMR.[27] The program yields binding constants K_1, $K_1 \cdot K_2$, and limiting chemical shifts.

Crystallographic Investigation. The relevant details of the crystals, data collection, and structure refinement can be found in Tables 2–4. Data collections for all compounds have been measured at low temperature using Mo Kα radiation. The used equipment was an Oxford Diffraction Sapphire/KM4 CCD (**1**, **2**, **3**, **6**) and a Bruker APEX II CCD (**4**, **5**, **7**) having both kappa geometry goniometers. Data were reduced by Crysalis PRO[28] (**1**, **2**, **3**, **6**) and EvalCCD[29] (**4**, **5**, **7**). Semiempirical[30] absorption correction was applied to all data sets. Structure solutions, refinements, and geometrical calculations have been carried out by SHELXTL.[31] All structures were refined using the full-matrix least-squares on F^2 with all non-H atoms anisotropically defined. The hydrogen atoms were placed in calculated positions using the "riding model" with $U_{iso} = a^*U_{eq}$ (where *a* is 1.5 for $-CH_3$ and $-OH$ moieties and 1.2 for others). All structures, except **1** and **7**, have been treated by the SQUEEZE[32] algorithm to take into account the electron density caused by a very disordered solvent and a missing F^- (**5** and **6**). Disorder problems, dealing mostly with the C_5Me_4R moieties, have been treated using the split model and applying some restraints.

Acknowledgment. The work was supported by the Swiss National Science Foundation, by the COST action D31, by the Swiss State Secretariat for Education and Research and by the EPFL.

Supporting Information Available: X-ray crystallographic file in CIF format. This material is available free of charge via the Internet at http://pubs.acs.org.

IC800410X

(27) Hynes, M. J. *J. Chem. Soc., Dalton Trans.* **1993**, 311–312.

(28) *CrysAlis PRO*; Oxford Diffraction Ltd.: Abingdon, Oxfordshire, OX14 1 RL, U.K., 2007.

(29) Duisenberg, A. J. M.; Kroon-Batenburg, L. M. J.; Schreurs, A. M. M. *J. Appl. Crystallogr.* **2003**, *36*, 220–229.

(30) Blessing, R. H. *Acta Crystallogr., Sect. A* **1995**, *51*, 33–38.

(31) SHELXTL 6.1.4; Sheldrick, G. M., *University of Göttingen: Göttingen, Germany, 1997*; Bruker AXS, Inc.: Madison, WI, 2003.

(32) Sluis, P. V. D.; Spek, A. L. *Acta Crystallogr., Sect. A* **1990**, *46*, 194–201.